

Regular paper

Electromagnetic coupling suppression of eight-ports MIMO antenna for satellite communication with neutralize block and parasitic elements

Muhammad Irshad Khan ^{a,*}, Shaobin Liu ^a, Jianliang Mao ^b, Abdul Basit ^c, Afzal Ahmed ^a, Amil Daraz ^c

^a College of Electronics and Information Engineering, Nanjing University of Aeronautics and Astronautics (NUAA), Nanjing 211106, China

^b College of Automation Engineering, Shanghai University of Electric Power, Shanghai 200090, China

^c School of Information Science and Engineering, Ningbotech University Ningbo 315100, China

ARTICLE INFO

Keywords:

DGS
MIMO
Mutual coupling
Neutralize block
Parasitic elements

ABSTRACT

In this article, eight elements multiple inputs and multiple outputs (MIMO) antenna for satellite communication with neutralize block, parasitic elements and Defective ground structure (DGS) is proposed. The proposed design is printed on FR4 low cost material with the size of 60 mm × 60 mm × 1.6 mm. The presented MIMO antenna contain four unit cells, four parasitic elements and DGS; each unit cell contain two radiating elements and neutralize block. Parasitic elements, DGS and neutralize block are used to minimize mutual coupling, neutralize block and parasitic elements are used on front side and DGS is on back side of the design. The reflection coefficient <-10 dB in the range of 14 GHz–18 GHz with impedance bandwidth of 4 GHz and isolation >25 dB in the given bandwidth. The envelope correlation coefficient (ECC) < 0.008, diversity gain (DG) > 9.96 dB and peak gain is equal to 6.32dBi. Furthermore the fabricated prototype was tested in anechoic chamber; measured results was analyzed and found similar to simulated results.

1. Introduction

Satellite communication is the integral part of wireless communication in current days. The demand of high data rate and gain increased day to day in wireless communication systems. Various techniques have been used, in order to maximize and support data rate. MIMO antenna systems attained much popularity in satellite communication due to the capability to achieve high data rates without using extra radiating power and frequency [1,2]. MIMO diversity antennas are also used for the support and improvement of multipath fading by using different diversity techniques such as pattern, space and polarization [3]. MIMO antennas have also some challenges in application on both sides (transmission and receiving) of communication such as antenna size and mutual coupling due to small gap between elements [4,5].

MIMO antenna systems are used for 4G, 5G, WLAN, WiMAX, UWB and satellite communication, in MIMO antennas there are various combination but most applicable are two ports MIMO antennas with decoupling stub for isolation [6–13], four ports with split-ring resonator, meandering technique and reflector for isolation [14–17], and eight element combination with various techniques [18–35]. The author

suggested eight ports antenna with minimum isolation of 15.5db and the size is 70 mm × 70 mm × 0.8 mm for UWB application [18]. In [19], eight elements antenna is recommended with overall mutual coupling of -20 dB, ECC is 0.08 and dimension is 40 mm × 40 mm × 40 mm. In [20], eight ports antenna for 5G communication is presented with poor isolation of 15 dB, ECC is 0.15 and overall size is 160 mm × 68 mm × 0.8 mm; decoupling stub is used for isolation. The author recommended MIMO antenna with strong mutual coupling of -15 dB and large size of 75 mm × 150 mm × 1.6 mm [21]. In [22], the author recommended eight-port antenna with poor isolation of 17.5 dB, ECC < 0.05 and size is 150 mm × 80 mm × 0.8 mm. The author recommended eight elements polarized antenna with very poor isolation of 8 dB and size of 70 mm × 70 mm × 0.8 mm [23]. The author designed eight elements dual polarized antenna with poor isolation of 12.5 dB, the size is 68 mm × 136 mm × 1 mm and the antenna is used for 4G communication [24]. In [25], the author designed eight ports antenna with the volume of 85 mm × 85 mm × 0.8 mm, the design has very poor isolation of 15 dB, ECC of 0.2 and poor gain of 2 dB.

The author recommended eight ports antenna with the size of 102 mm × 52 mm × 1.6 mm for WLAN application, minimum isolation is

* Corresponding author.

E-mail address: irshadnawab@nuaa.edu.cn (M.I. Khan).

Table 1

Comparison of proposed design with literature cited.

Ref.	Size (mm ³)	ports	Decoupling Techniques/Ground	Isolation (dB)	ECC	DG (dB)
[23]	70 × 70 × 0.8	8	Without/connected	>8	<0.1	-
[24]	68 × 136 × 1	8	Without/connected	>12.5	<0.15	-
[25]	85 × 85 × 0.8	8	DGS/connected	>15	<0.2	-
[26]	102 × 52 × 1.6	8	Without/not connected	>15	<0.5	9
[27]	68 × 68 × 21.6	8	Without/not connected	>18	<0.025	9.9
[28]	144 × 69 × 1.6	8	Parasitic element/connected	>18	<0.36	9.5
[29]	27.4 × 27.4 × 1.6	3	Without/connected	>18	<0.02	-
[30]	174 × 85 × 0.8	8	Without/connected	>13.8	<0.025	-
[31]	150 × 75 × 0.8	8	Neutralize line/connected	>11.5	<0.08	-
[32]	150 × 75 × 0.8	8	Without/connected	>11	<0.1	-
[33]	60 × 60 × 50	8	Without/not connected	>20	<0.01	9.98
[34]	120.75 × 120.75 × 9	8	Without/connected	>20	<0.03	-
This work	60 × 60 × 1.6	8	Hybrid techniques/connected	>25	<0.008	9.96

Table 2

Dimensions of proposed MIMO antenna for satellite communication.

Dimensions	Value (mm)	Dimensions	Value (mm)
W	36	L	18
w_p	7	l_p	3.6
w_f	1.6	l_f	5.25
w_{inset}	0.6	l_{inset}	2.25
w_{slot}	5.6	l_{slot}	1.8
w_1	0.4	l_1	2.9
w_{bl}	7	l_{bl}	5
d_{gap}	8	l_2	2.2

15db, DG is >9 and ECC < 0.5 [26]. In [27], eight elements antenna is recommended with poor isolation of 18 dB, ECC is 0.025 and dimension is 68 mm × 68 mm × 21.6 mm. In [28], eight ports antenna for 5G communication is presented, poor isolation is 18 dB, high ECC is 0.36, size is 160 mm × 68 mm × 0.8 mm, and parasitic element is used for isolation. The author suggested three ports antenna for satellite communication with the size of 27.4 mm × 27.4 mm × 1.6 mm, maximum mutual coupling is -18 dB [29]. In [30], the author recommended eight port antenna with poor isolation of 13.8 dB, ECC < 0.025, the size is 174 mm × 85 mm × 0.8 mm and CSRR is used for isolation. The author recommended eight elements antenna with size of 150 mm

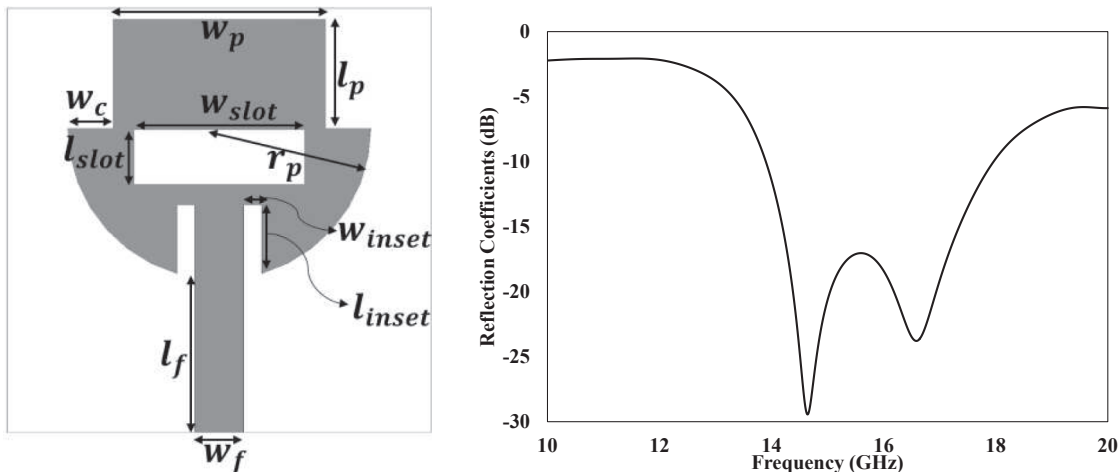


Fig. 1. Single port design for satellite communication (a) design (b) reflection coefficient.

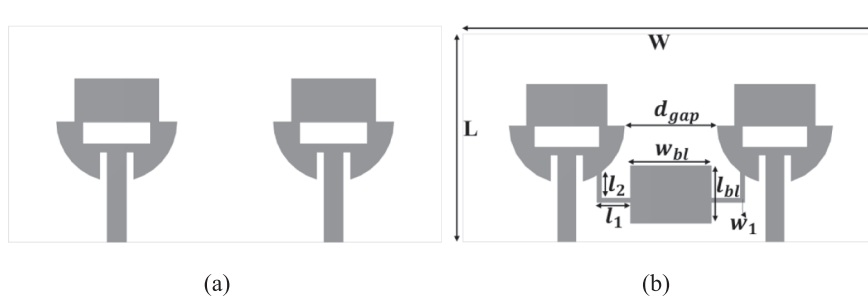


Fig. 2. Two ports antenna for satellite communication (a) without neutralize block (b) with neutralize block.

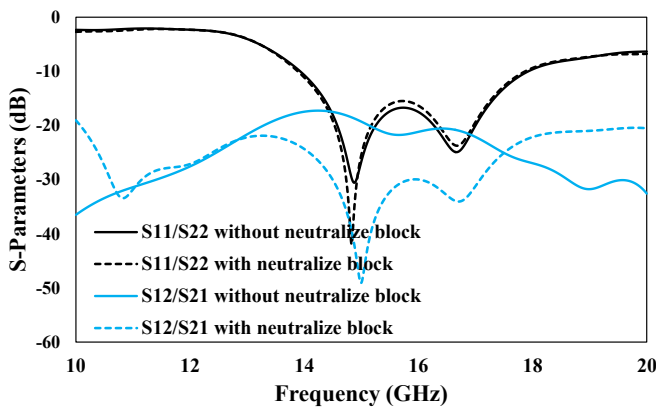


Fig. 3. S-parameters of two ports design.

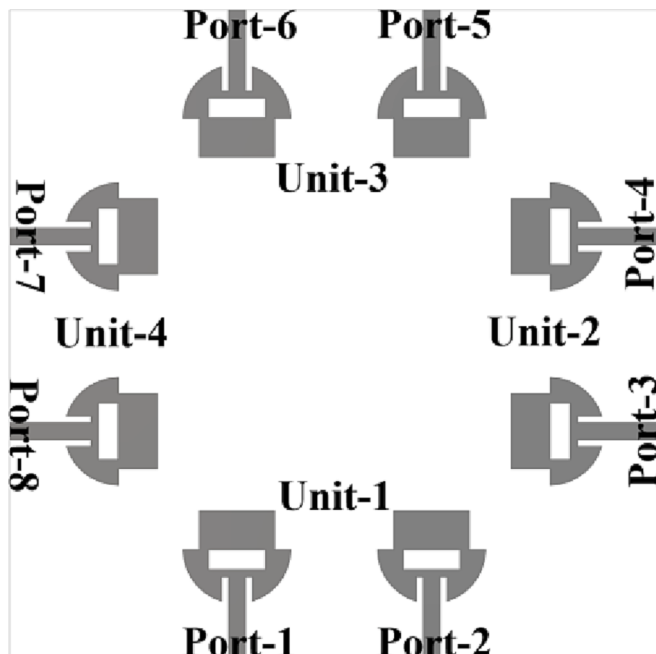


Fig. 4. Eight ports antenna without decoupling structure.

$\times 75 \text{ mm} \times 0.8 \text{ mm}$, ECC is <0.08 [31]. The author designed eight elements antenna with poor isolation of 11 dB, the size is $150 \text{ mm} \times 75 \text{ mm} \times 0.8 \text{ mm}$ and the antenna is used for 5G communication [32]. In [33], the author designed eight ports antenna with the volume of $60 \text{ mm} \times 60 \text{ mm} \times 50 \text{ mm}$, the design has isolation of 20 dB, ECC of 0.01 and poor gain of 2 dB. The author recommended eight ports four elements antenna with the size of $120.75 \text{ mm} \times 120.75 \text{ mm} \times 9 \text{ mm}$ for WLAN and WiMAX (2.4 GHz and 3.5 GHz) application, minimum isolation is 20db [34]. In [35], eight elements MIMO antenna is presented with dimension of $30 \text{ mm} \times 60 \text{ mm} \times 0.8 \text{ mm}$, the design has poor isolation of 11.5 dB and ECC is 0.2, modal currents cancelation techniques is used for isolation. In [36], eight elements/twelve ports antenna for UWB communication is presented, overall size is $33 \text{ mm} \times 33 \text{ mm} \times 15 \text{ mm}$, ECC is 0.5 and minimum isolation is 15 dB. In [37], four/eight ports antenna is recommended, the overall size of eight port antenna is $90 \text{ mm} \times 90 \text{ mm} \times 1.6 \text{ mm}$, ECC < 0.015 , peak gain is equal to 4.5 dB and

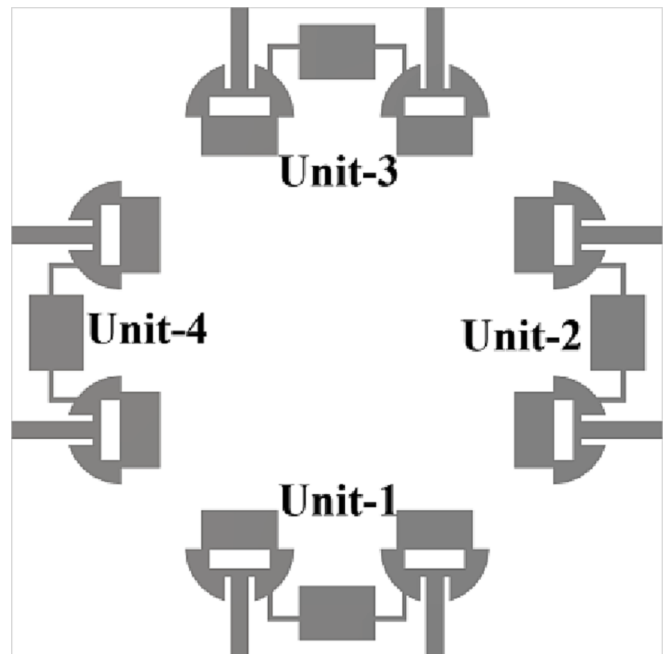
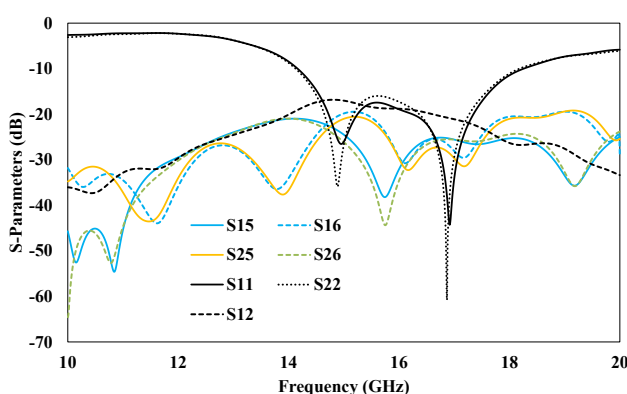
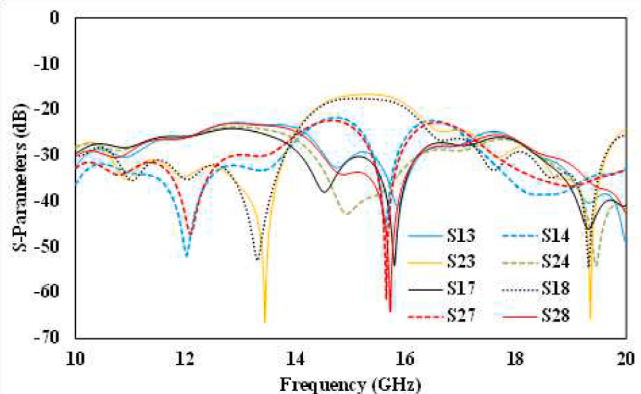


Fig. 6. Eight ports MIMO antenna with neutralize blocks.



(a)



(b)

Fig. 5. S-parameters of eight ports antenna without decoupling structure (a) Unit-1 and Unit-3 (b) Unit-1, Unit-2 and Unit-4.

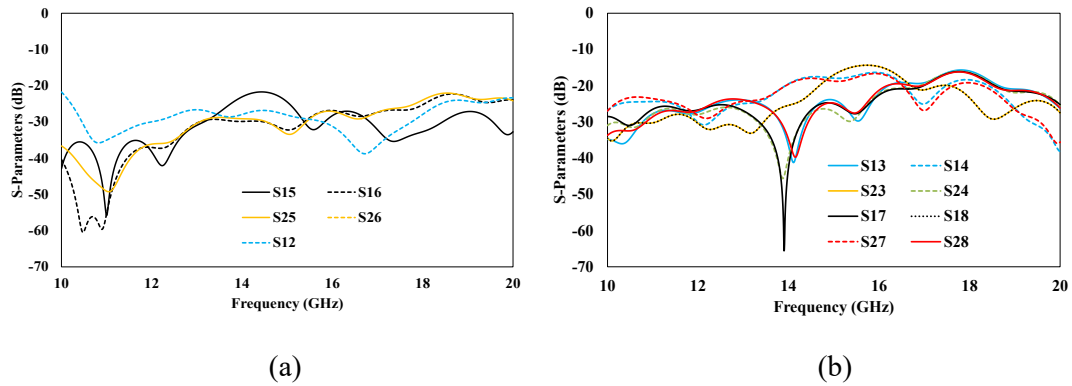


Fig. 7. Mutual coupling of MIMO antenna with neutralize blocks (a) Unit-1 and Unit-3 (b) Unit-1, Unit-2 and Unit-4.

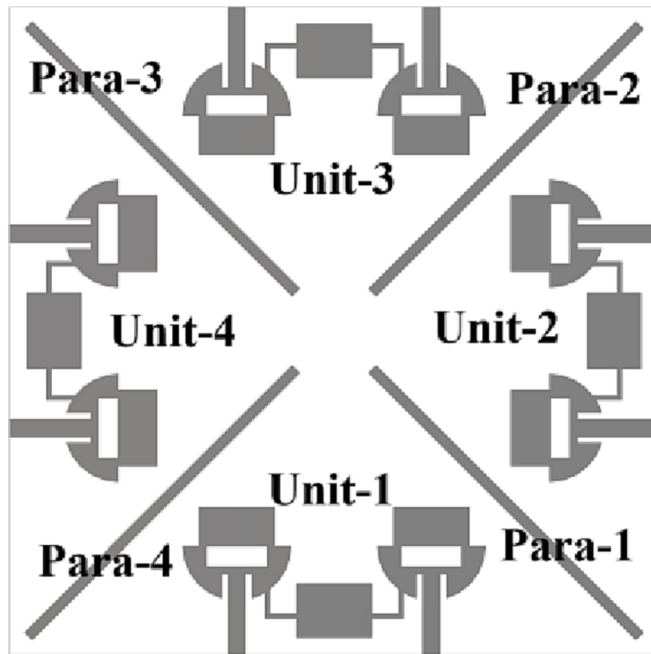


Fig. 8. Eight ports MIMO antenna with neutralize blocks and parasitic elements.

isolation >15 dB, the comparison of most relevant literature with presented design are also mention in tabular form in Table 1.

In the above literature, most of the design have minimum isolation due to use of single decoupling techniques, complex circuitry due to isolation techniques, large size, DG and ECC is calculated from S-parameters, most of the designs are presented for lower frequency bands and some of the designs have non-connected grounds and without decoupling techniques. So keeping the aforementioned challenges, the author proposed simple structured MIMO antenna system with novel neutralize block, parasitic elements and DGS for satellite communication. The reflection coefficient <-10 dB in the range of 14 GHz–18 GHz with impedance bandwidth of 4 GHz and mutual coupling <-25 dB in the given bandwidth. The ECC < 0.008 , DG > 9.96 dB and calculated from far field results. The proposed design has novel hybrid techniques for high isolation, compact size, low ECC and high DG and peak gain in comparison with literature cited.

2. Antenna design and characterization

The presented antenna for satellite communication is printed on FR4 low cost material. The overall size of eight ports design is $60\text{ mm} \times 60\text{ mm} \times 1.6\text{ mm}$. The novel neutralize block, DGS and parasitic elements are introduce to minimize mutual coupling. The fabricated design was tested in anechoic chamber and vector network analyzer.

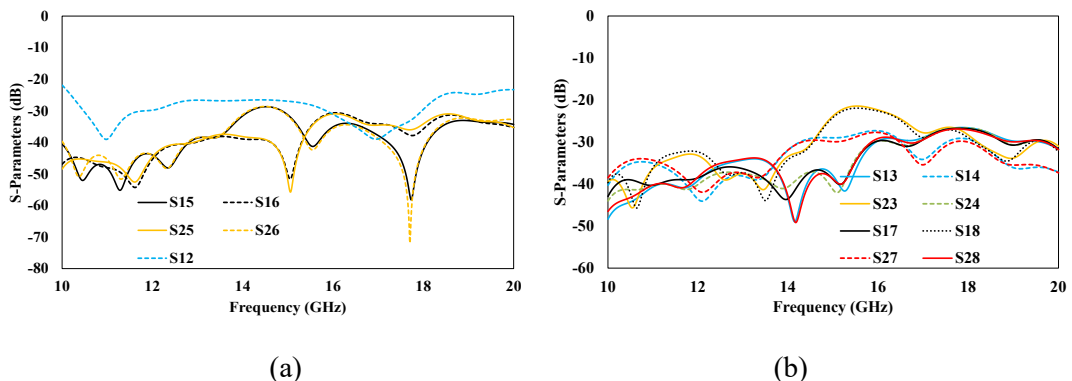


Fig. 9. Mutual coupling of eight elements antenna with neutralize blocks and parasitic elements (a) Unit-1 and Unit-3 (b) Unit-1, Unit-2 and Unit-4.

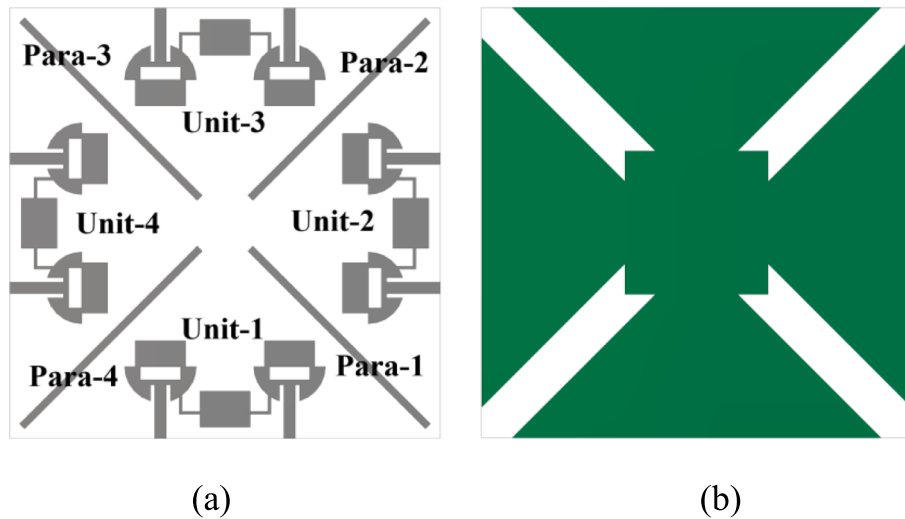


Fig. 10. Proposed eight ports MIMO antenna (a) front side (b) back side.

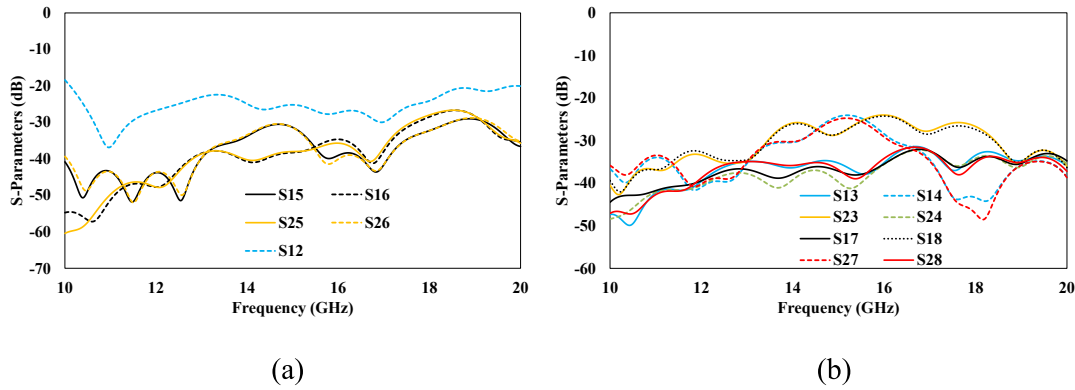


Fig. 11. Mutual coupling of proposed MIMO antenna (a) Unit-1 and Unit-3 (b) Unit-1, Unit-2 and Unit-4.

2.1. Two ports MIMO antenna with novel neutralize block

The two ports design is basically the extension of single element antenna. Single radiating element contain rectangular and half circular patch. The size of the single port antenna is $14\text{ mm} \times 14\text{ mm} \times 1.6\text{ mm}$, the radius of half circular patch (r_p) is 5 mm, the size of rectangular patch ($l_p \times w_p$) is $3.6\text{ mm} \times 7\text{ mm}$ and the size of feed line ($l_f \times w_f$) is $5.25\text{ mm} \times 1.6\text{ mm}$. The slot is etched in the center of radiating patch with the dimension of $1.8\text{ mm} \times 5.6\text{ mm}$ ($l_{slot} \times w_{slot}$). Similarly the dimension of two ports antenna is $18\text{ mm} \times 36\text{ mm} \times 1.6\text{ mm}$, the size of neutralize block is $5\text{ mm} \times 7\text{ mm}$ ($l_b \times w_b$), the width and length of connected line between neutralize block and radiating patch is 0.4 mm (w_1) and $2.9\text{ mm} + 2.2\text{ mm}$ ($l_1 + l_2$) respectively. The distance between two radiating elements is 8 mm (d_{gap}); various other dimensions are mentioned in detail in [Table 2](#). The radius of radiating patch is estimated from equations [\(1\)](#) and [\(2\)](#) [38]. Where ‘ a ’ is the radius of patch f_0 is resonance frequency, h is height of the substrate, ϵ_r is relative permittivity.

$$a = \frac{F}{\left\{ 1 + \frac{2h}{\pi \epsilon_F F} \left[\ln \left(\frac{\pi F}{2h} \right) + 1.7726 \right] \right\}^{1/2}} \quad (1)$$

$$F = \frac{8.791 \times 10^9}{f_o \sqrt{\epsilon_r}} \quad (2)$$

The design and reflection coefficient of single radiating element are illustrated in Fig. 1. The radiating elements is fed with inset feeding and the reflection coefficient <-10 dB in the range of 14 GHz–18 GHz with impedance bandwidth of 4 GHz. The two elements antenna without and with neutralize block are shown in Fig. 2. The mutual coupling is improved from -16 dB to -30 dB which is very good achievement for two elements MIMO antenna and S_{11}/S_{22} are almost similar in both cases; illustrated in Fig. 3.

2.2. Proposed MIMO antenna with novel neutralize block, parasitic elements and DGS

The eight ports antenna for satellite communication is essentially the extended version of two elements antenna. The presented eight elements antenna contain four unit cells, four parasitic elements and DGS; each unit cell contain two radiating elements and neutralize block. Parasitic elements are placed diagonally on front side; the size of each parasitic element is $35\text{ mm} \times 0.8\text{ mm}$. Similarly DGS is introduced on back side by cutting the ground diagonally with the width of 6 mm and finally square patch is placed in the center with each side of 20 mm to connect all four parts of ground. Neutralize blocks are used for the decoupling of inter-units elements such as element-1 and element-2, element-3 and element-4, element-5 and element-6, element-7 and element-8. Similarly Para-1 is introduced to minimize coupling between unit-1 and unit-

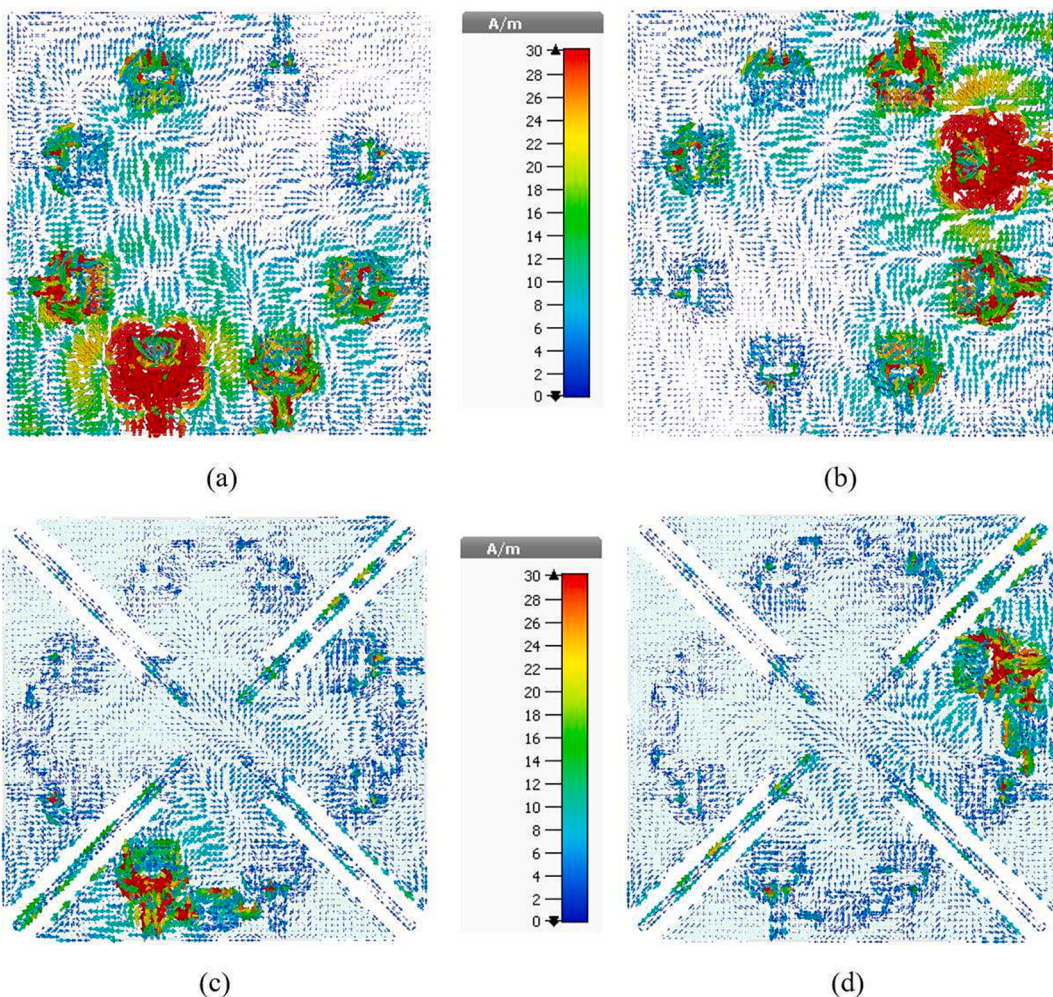


Fig. 12. Current distribution of presented design at 15 GHz (a) element-1 excited without decoupling techniques (b) element-4 excited without decoupling techniques (c) element-1 excited with decoupling structure (d) element-4 excited with decoupling structure.

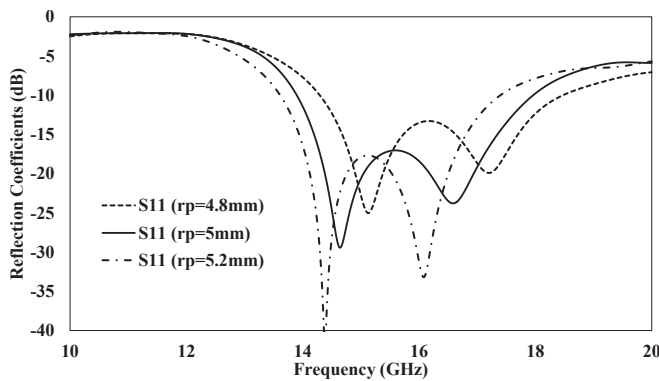


Fig. 13. Simulated reflection coefficients by changing the radius of radiating patch.

2, Para-2 minimized coupling between unit-2 and unit-3, Para-3 minimized coupling between unit-3 and unit-4, Para-4 minimized coupling between unit-4 and unit-1. DGS is used for isolation enhancement in both adjacent units and opposite units.

The proposed design for satellite communication is evaluated and analyzed in various steps, step-I is without decoupling techniques, step-II is with neutralize block, step-III is with neutralize block and parasitic elements and step-IV is presented design. The eight elements antenna without decoupling techniques is shown in Fig. 4. The reflection

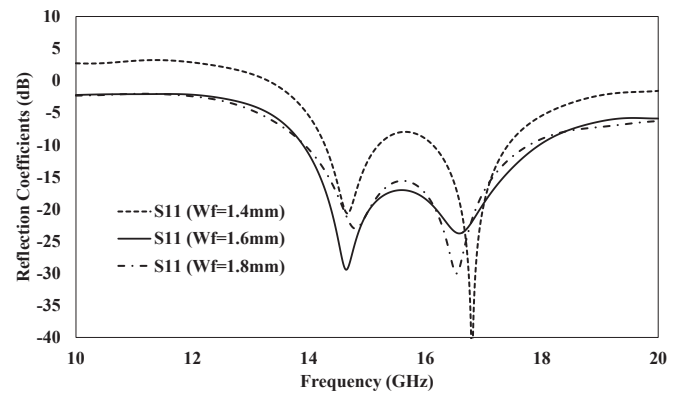


Fig. 14. Simulated reflection coefficients by varying the feed line width.

coefficients are less than -10 dB in the range of 14 GHz–18 GHz with impedance bandwidth of 4 GHz and mutual coupling is less than -14 dB in both opposite and adjacent units; justified from Fig. 5. In step-II, the neutralize block is added to step-I, shown in Fig. 6, the inter-unit mutual coupling is improved and reach -25 dB in given range; justified from Fig. 7(a). The opposite and adjacent mutual coupling is almost same to step-I; justified from Fig. 7. In step-III the parasitic elements are added to step-II, shown in Fig. 8. The parasitic elements improved the mutual coupling from -15 dB to -22 dB in the adjacent unit cell and also

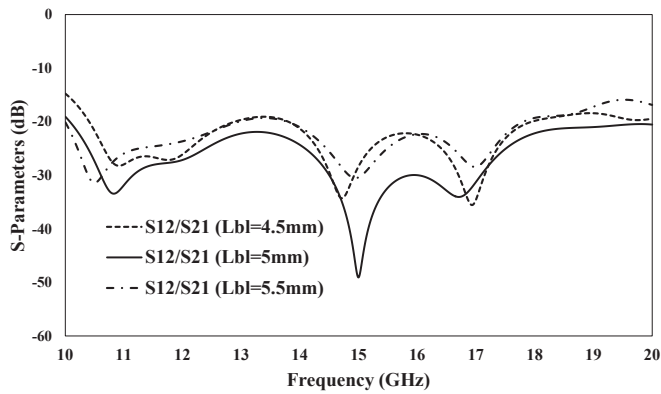


Fig. 15. S-parameters by changing the length of neutralize block.

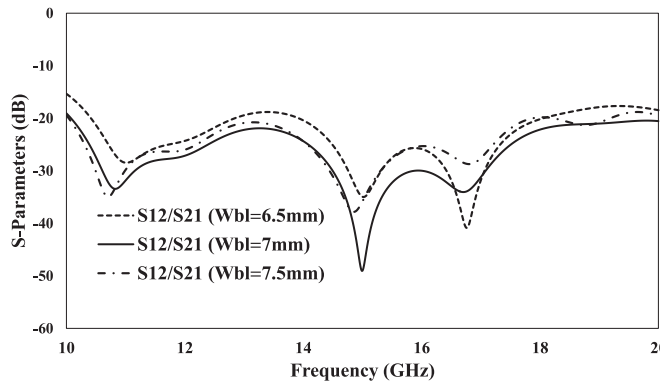


Fig. 16. S-parameters by changing the width of neutralize block.

improved mutual coupling of opposite units little bit; justified from Fig. 9. In step-IV the DGS is introduced to existing design of step-III to form proposed design with hybrid techniques; shown in Fig. 10. The DGS improved the isolation of opposite units and add small contribution to adjacent units. The cumulative mutual coupling is less than -25 dB in both opposite and adjacent units; justified from Fig. 11.

Current distribution is also presented to investigate and analyze isolation mechanism, where port-1 and port-4 are excited for better understanding and investigation. The current distribution at 15 GHz are shown in Fig. 12. In Fig. 12(a) and Fig. 12(b), most of the current are found on element-1 and element-4, which are excited ports and strong mutual coupling occurred also between excited elements and remaining elements due to without decoupling structure. Similarly in Fig. 12(c) and Fig. 12(d) most current are distributed on excited elements and decoupling structure such as neutralize block, parasitic elements and DGS.

2.3. Parametric evaluation and analysis

Various dimension parameters such as feed line, radius of radiating patch, width of DGS, length and width of neutralized block are evaluated and analyzed in term of reflection coefficients, mutual coupling and impedance bandwidth. The effect on reflection coefficients due change in radius of radiating patch is shown in Fig. 13, by increasing the radius (r_p) of the patch, the reflection coefficient moved to lower frequencies and similarly by decreasing the radius, the reflection coefficient moved to higher frequencies. The feed line width (w_f) is most critical part of antenna, the impedance mismatch occurred by varring feed line by 2

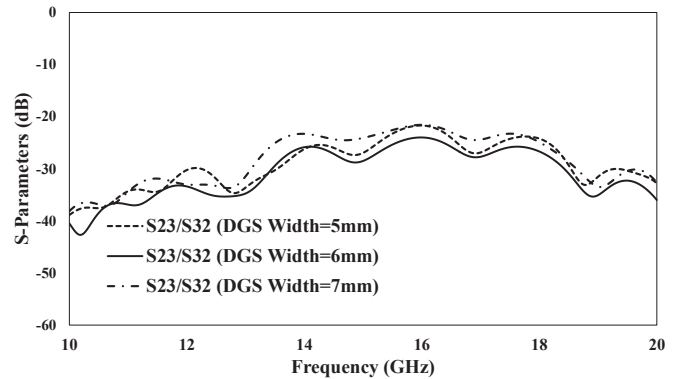


Fig. 17. S-parameters by changing the width of DGS.

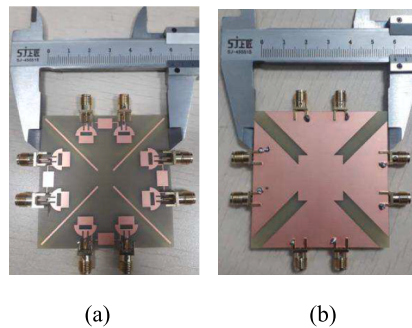


Fig. 18. Fabricated image of proposed design (a) top view (b) bottom view.

mm and the reflection coefficient has better response at $w_f = 1.6$ mm clearly justfied from Fig. 14. The neutralize block is also evaluated in term of length (L_{bl}) and width (w_{bl}), by changing the length of neutralized block the response of mutual coupling became poor clearly justified from Fig. 15, similarly by changing the width of ntralize block the response of mutual coupling is relatively better at $w_{bl} = 7$ mm; depicted in Fig. 16. The S-parameters due to change in width of DGS is depicted in Fig. 17. The response of mutual coupling is relatively better at DGS width = 6 mm as compared to remain values.

3. Results and discussion

The proposed design have eight radiating elements, four parasitic elements and defective ground. The prototype image of proposed antenna is shown in Fig. 18 and experimental and simulated results are illustrated in Fig. 19. The reflection coefficient <-10 dB in the range of 14 GHz–18 GHz with impedance bandwidth of 4 GHz and mutual coupling <-25 dB in the given bandwidth, a small shift towards high frequency is noted in reflection coefficient and small changes are noted also in mutual coupling with simulated results. The XZ-plane (E-plane, $\phi = 0$) and YZ-plane (H-plane, $\phi = 90^\circ$) radiation patterns at 15 GHz and 16.5 GHz are illustrated in Fig. 20. In Fig. 20(a), the intensity of radiation occurred at 30° and 300° in XZ-plane, the null radiation noted at 120° and similarly the intensity of radiation occurred at 0° – 30° and 330° – 360° and the null radiation noted at 170° in YZ-plane. In Fig. 20 (b), the intensity of radiation noted at 0° – 30° in both XZ and YZ planes, the null radiation in XZ-plane noted at 120° and 210° and similarly the null radiation in YZ-plane noted at 130° , the level of side lobes are minimum in both Planes. The co-polarization is much higher than cross-polarization, the value of cross-polarization is below -20 dB at both

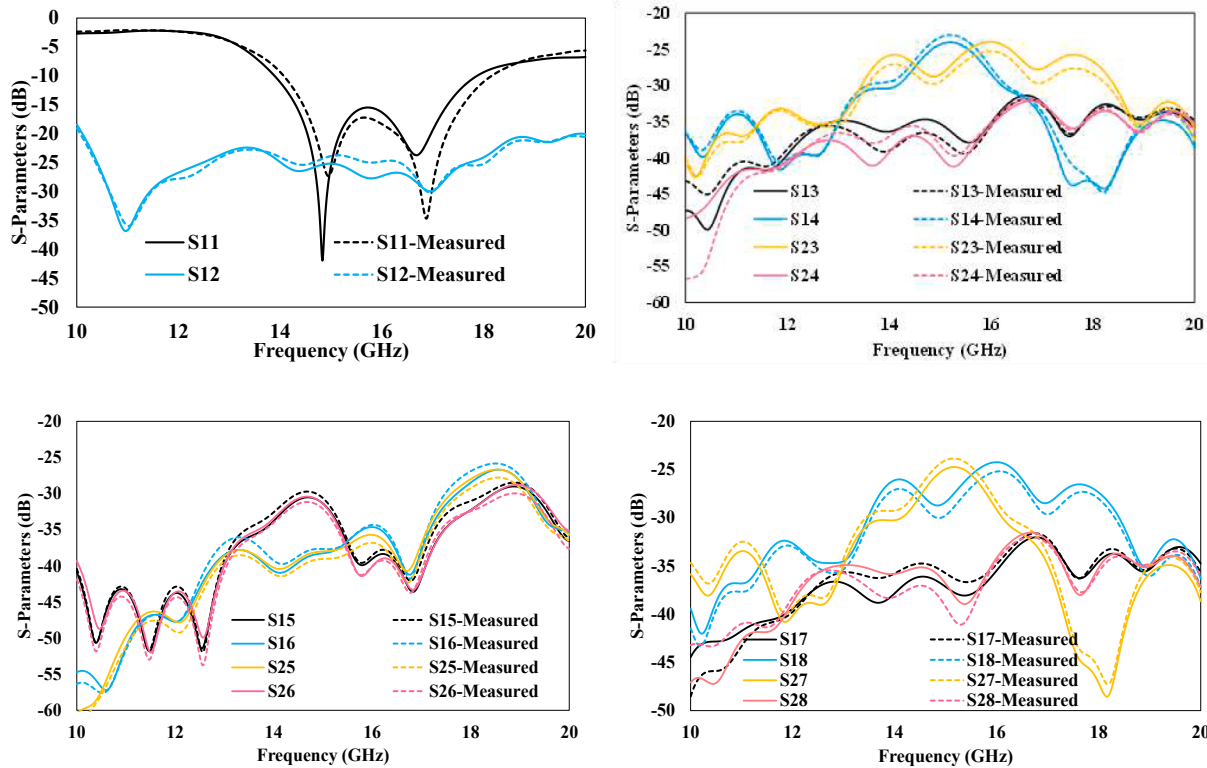


Fig. 19. S-parameters of proposed design for satellite communication (a) Port-1 and Port-2 (b) Unit-2 and Unit-1 (c) Unit-3 and Unit-1 (d) Unit-4 and Unit-1.

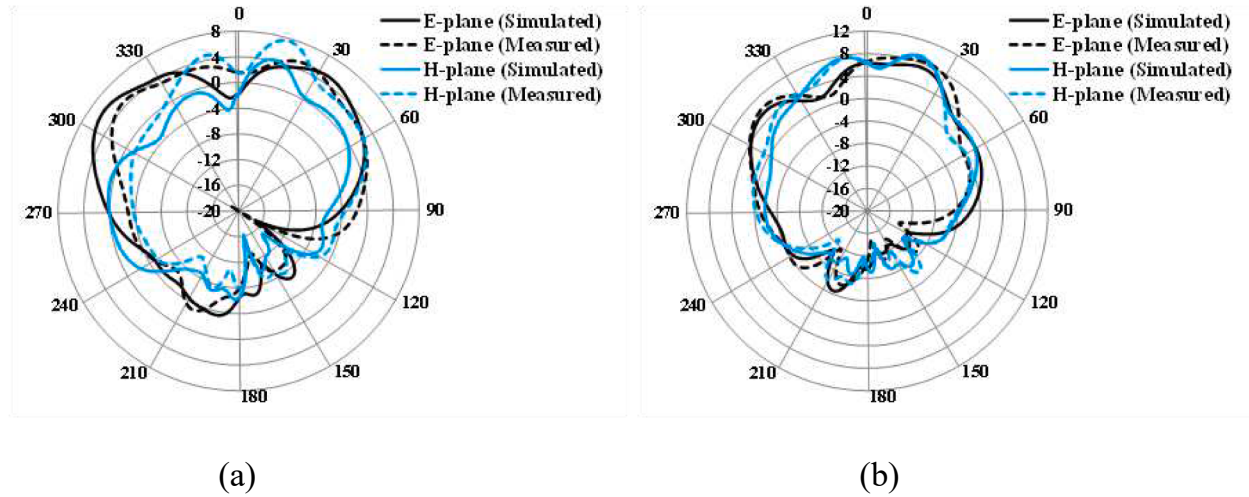


Fig. 20. Radiation pattern of presented antenna (a) 14.5 GHz (b) 16.5 GHz.

frequencies; clearly justified from Fig. 21.

Diversity performance is investigated from DG, ECC and multiplexing efficiency, both the S-parameters and radiation pattern are used to calculate ECC and DG but most acceptable and reliable method is radiation pattern, equations (3) and (4) are used to calculate ECC and DG from radiation pattern [39].

$$ECC = \frac{\left| \iint_{4\pi} \overrightarrow{F}_i(\theta, \phi)^* \overrightarrow{F}_j(\theta, \phi) d\Omega \right|^2}{\iint_{4\pi} |\overrightarrow{F}_i(\theta, \phi)|^2 d\Omega \iint_{4\pi} |\overrightarrow{F}_j(\theta, \phi)|^2 d\Omega} \quad (3)$$

$$DG = 10 \sqrt{1 - (ECC)^2} \quad (4)$$

$\overrightarrow{F}_i(\theta, \phi)$ and $\overrightarrow{F}_j(\theta, \phi)$ are farfield radiation pattern due to i^{th} and j^{th} elements in N-elements MIMO system. The simulated ECC < 0.008 , measured ECC < 0.035 and DG $> 9.96\text{dB}$ in the given band; as shown in Fig. 22. Multiplexing efficiency is usually considered as the total efficiency, but it is not only the total efficiency, but also includes efficiency imbalance and correlation. Multiplexing efficiency is less than -2dB , multiplexing efficiency is calculated from equation (5) [40], radiation efficiency is greater than multiplexing efficiency; justified from Fig. 23.

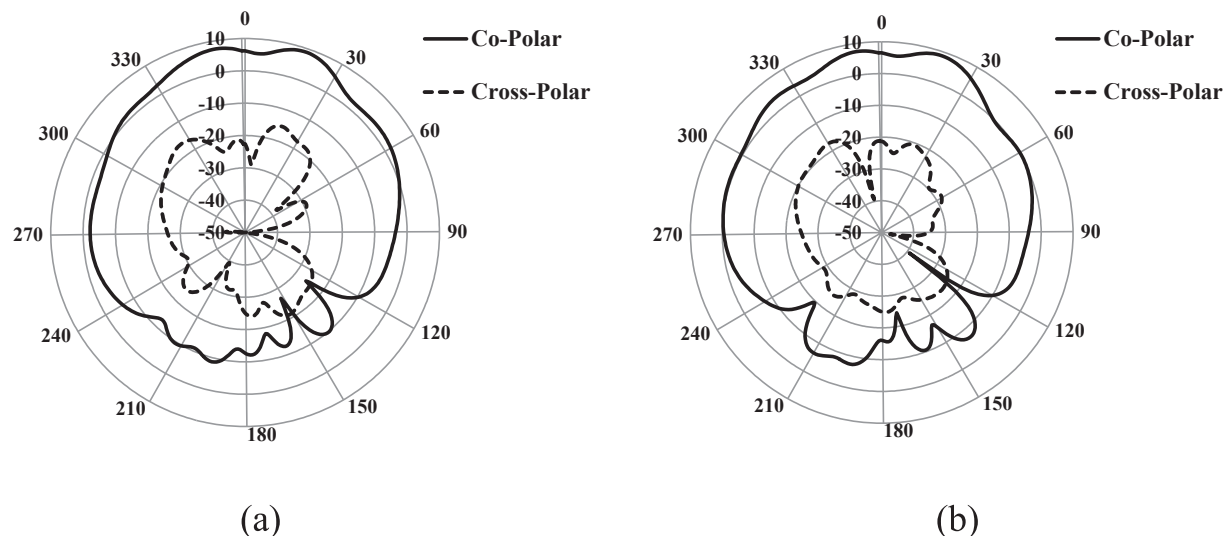


Fig. 21. Co and cross polarization pattern of presented antenna (a) 14.5 GHz (b) 16.5 GHz.

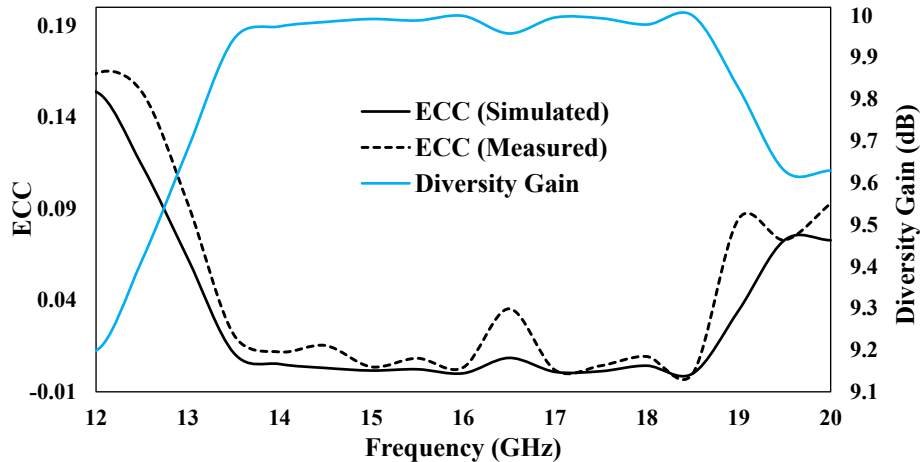


Fig. 22. DG and ECC of presented antenna for satellite communication.

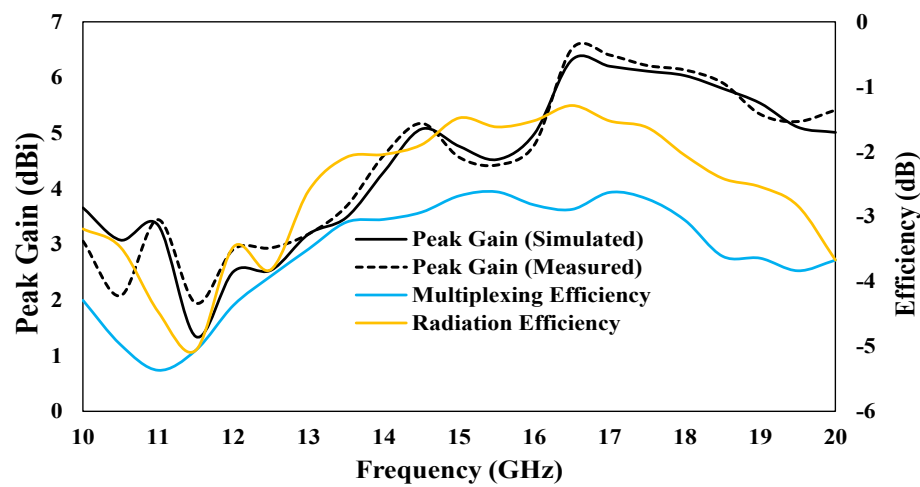


Fig. 23. Multiplexing efficiency, Radiation efficiency and Peak gain of MIMO antenna for satellite communication.

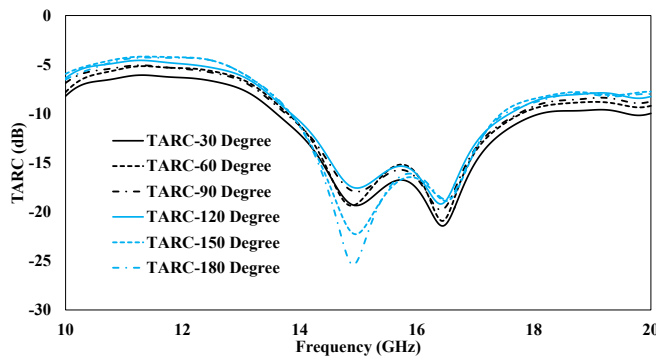


Fig. 24. TARC performance of proposed MIMO antenna for satellite communication.

Simulated and tested peak gain is nearly same and equal to 6.32dBi in the required bandwidth; illustrated in Fig. 18.

$$\eta_{max} = \sqrt{\eta_i \eta_j (1 - |\rho_c|^2)} \quad (5)$$

The complex correlation coefficients $\rho_c(i, j, N)$ is related to the ECC $\rho_e(i, j, N)$ for (i, j) th elements of MIMO antenna, such as $\rho_c(i, j, N) = |\rho_e(i, j, N)|^{1/2}$.

Total active reflection coefficient (TARC) is also one of the basic evaluating parameter of MIMO performance. TARC is basically the ratio of the square root of reflected power to the square root of incident power. Reflected power equal to incident power provided by all ports minus total radiated power. TARC is calculated from equation (6) using scattering matrix [41]. Where $|b_k|$ and $|a_k|$ are exciting and scattering vectors. The effect of TARC on bandwidth is verified and shown in Fig. 24, the TARC values are lower than -10 dB in required bandwidth for all angle varied from 30° to 180° . Channel capacity loss (CCL) and mean effective gain (MEG) are also important parameters to evaluate the quality of MIMO antenna, in practical model the minimum value of CCL is 0.5 bits/sec/Hz and the minimum acceptable value MEG is below

-3 dB for quality communication. The CCL is <0.25 bits/sec/Hz and MEG is less than -3 dB in the required bandwidth; clearly justified from Fig. 25.

$$TARC = \frac{\sqrt{\sum_{k=0}^n (|b_k|^2)}}{\sqrt{\sum_{k=0}^n (|a_k|^2)}} \quad (6)$$

4. Conclusion

In this paper, MIMO antenna with novel neutralize block, parasitic elements and DGS for satellite communication is proposed. The proposed design is printed on FR4 low cost material. DGS, parasitic elements and neutralize block are used to minimize mutual coupling, neutralize block and parasitic elements are used on front side and DGS is use on back side of proposed eight ports MIMO design. The eight ports antenna for satellite communication is essentially the extended version of two elements antenna. The presented eight elements antenna contain four unit cells, four parasitic elements and DGS; each unit cell contain two radiating elements and neutralize block. The reflection coefficient <-10 dB in the range of 14 GHz–18 GHz with impedance bandwidth of 4 GHz and mutual coupling <-25 dB in the given bandwidth. The presented eight elements MIMO antenna is suitable for satellite communication after experimental investigation of S-parameter, peak gain, ECC, DG and multiplexing efficiency.

Declaration of Competing Interest

The authors declare that they have no known competing financial interests or personal relationships that could have appeared to influence the work reported in this paper.

Data availability

No data was used for the research described in the article.

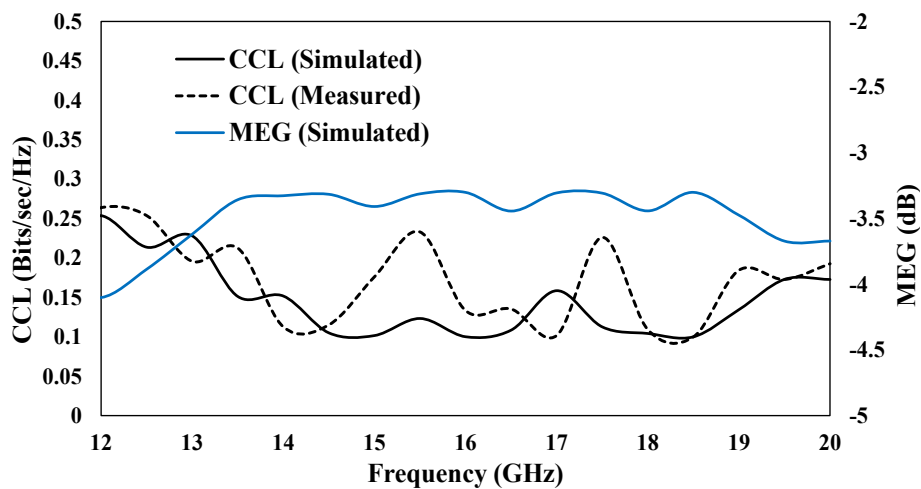


Fig. 25. CCL and MEG of proposed MIMO antenna for satellite communication.

References

- [1] Andrews JG, Buzzi S, Choi W, Hanly SV, Lozano A, Soong AC, et al. What will 5G be? *IEEE J Sel Areas Commun* 2014;32(6):1065–82.
- [2] Chattha HT, Ishfaq MK, Khawaja BA, Sharif N. Compact multiport MIMO antenna system for 5G IoT and cellular handheld applications. *IEEE Antennas Wirel Propag Lett* 2021;20(11):2136–40.
- [3] Mattheijssen P, Herben M, Dolmans G, Leyten L. Antenna-pattern diversity versus space diversity for use at handhelds. *IEEE Trans Veh Technol* 2004;53(4):1035–42.
- [4] Foschini G, Gans MJ. On limits of wireless communications in a fading environment when using multiple antennas. *Wireless Pers Commun* 1998;6(3): 311–35.
- [5] Kildal PS, Rosengren K. Correlation and capacity of MIMO systems and mutual coupling, radiation efficiency and diversity gain of their antennas: simulations and measurements in a reverberation chamber. *IEEE Commun Mag* 2004;42(12): 104–12.
- [6] Khan MI, Khattak MI, Al-Hasan M. Miniaturized MIMO antenna with low inter-dipole transmittance and band rejection features. *J Electromagn Eng Sci* 2021;21(4):307–15.
- [7] Khan MK, Feng Q. Design and experimental validation of UWB MIMO antenna with triple band-notched characteristics. *Prog Electromagn Res C* 2021;116:51–64.
- [8] Zhang L, Feng Q, Khan MK. Design of a novel circularly polarized MIMO antenna with enhanced isolation for ultra-wideband communication. *Appl Comput Electromagn Soc J (ACES)* 2022;607–18.
- [9] Khattak MI, Khan MI, Anab M, Ullah A, Al-Hasan M, Nebhen J. Miniaturized CPW-fed UWB-MIMO antennas with decoupling stub and enhanced isolation. *Int J Microw Wireless Technol* 2022;14(4):456–64.
- [10] Sharma M, Gautam AK, Agrawal N, Singh N. Design of MIMO planar antenna at 24 GHz band for radar, communication and sensors applications. *AEU-Int J Electron Commun* 2021;136:153747.
- [11] Kumar P, Sinha R, Choubey A, Mahto SK. A miniaturized rectangular shape narrowband MIMO antenna with reduced mutual coupling for C-band applications. *J Electromagn Waves Appl* 2022;36(12):1717–30. <https://doi.org/10.1080/09205071.2022.2041492>.
- [12] Khan MI, Khattak MI. Designing and analyzing a modern MIMO-UWB antenna with a novel stub for stop band characteristics and reduced mutual coupling. *Microwave Opt Technol Lett* 2020;1–6. <https://doi.org/10.1002/mop.32425>.
- [13] Parchin NO, et al. Four-element/eight-port MIMO antenna system with diversity and desirable radiation for sub 6 GHz modern 5G smartphones. *IEEE Access* 2022; 10:133037–51. <https://doi.org/10.1109/ACCESS.2022.3227199>.
- [14] Rekha S, Jino Ramson SR. Parasitically isolated 4-element MIMO antenna for 5G/WLAN applications. *Arab J Sci Eng* 2022;47:14711–20. <https://doi.org/10.1007/s13369-022-06952-w>.
- [15] Karimian R, Soleimani M, Hashemi SM. Tri-band four elements MIMO antenna system for WLAN and WiMAX application. *J Electromagn Waves Appl* 2012;26 (17–18):2348–57. <https://doi.org/10.1080/09205071.2012.734433>.
- [16] Khan MI, Liu S, Kabir MI, Rahman SU. Eight elements MM-wave MIMO antenna for anti-collision radar sensing application with novel hybrid techniques. *AEU- Int J Electron Commun* 2023;167:1–10. <https://doi.org/10.1016/j.aeue.2023.154687>.
- [17] Saha PB, Dash RK, Ghoshal D. Triple-band four-port MIMO antenna with reduced mutual coupling using Minkowski-modified novel fractal loop. *Wireless Pers Commun* 2021;117(3):2253–71.
- [18] Saurabh AK, Dubey R, Meshram MK. Wideband eight-element MIMO antenna with band-dispersion characteristics. *AEU-Int J Electron Commun* 2022;155:1–11.
- [19] Mohanty A, Sahu S. 2-d printed 8-element compact UWB diversity antenna for multi-service-multi-mode applications. *AEU-Int J Electron Commun* 2022;151: 154215.
- [20] Nithya S, Seethalakshmi V. MIMO antenna with isolation enrichment for 5G mobile information. *Mob Inf Syst* 2022;2022:1802352. <https://doi.org/10.1155/2022/1802352>.
- [21] Parchin NO, et al. Eight-element dual-polarized MIMO slot antenna system for 5G smartphone applications. *IEEE Access* 2019;7:15612–22. <https://doi.org/10.1109/ACCESS.2019.2893112>.
- [22] Li Y, Sim C-Y-D, Luo Y, Yang G. High-isolation 3.5 GHz eight-antenna MIMO array using balanced open-slot antenna element for 5G smartphones. *IEEE Trans Antennas Propag* 2019;67(6):3820–30. <https://doi.org/10.1109/TAP.2019.2902751>.
- [23] Biswal SP, Das S. Eight-element-based MIMO antenna with CP behaviour for modern wireless communication. *IET Microw Antennas Propag* 2020;14:45–52. <https://doi.org/10.1049/iet-map.2019.0552>.
- [24] Li M-Y, et al. Eight-port orthogonally dual-polarized antenna array for 5G smartphone applications. *IEEE Trans Antennas Propag* 2016;64(9):3820–30. <https://doi.org/10.1109/TAP.2016.2583501>.
- [25] Mathur R, Dwari S. 8-port multibeam planar UWB-MIMO antenna with pattern and polarisation diversity. *IET Microw Antennas Propag* 2019;13:2297–302. <https://doi.org/10.1049/iet-map.2019.0134>.
- [26] Roy S, Ghosh S, Chakraborty U. Compact dual wide-band four/eight elements MIMO antenna for WLAN applications. *Int J RF Microwave Comput Aided Eng* 2019;29(7):e21749.
- [27] Srivastava K, Kumar S, Kanaujia BK, Dwari S, Choi HC, Kim KW. Compact eight-port MIMO/diversity antenna with band rejection characteristics. *Int J RF Microw Comput Aided Eng* 2020;30:e22170.
- [28] Narayana DL, Aruna S, Roy S, Naik KS. Eight element low-cost microstrip MIMO antenna for Wi-MAX and 5G applications. *Wireless Pers Commun* 2021;121(3): 1437–56. <https://doi.org/10.1007/s11277-021-08678-8>.
- [29] Satam V, Nema S. Compact, high gain, linearly polarized diversity antenna for KU band applications. *Microwave Opt Technol Lett* 2018;60:2843–9. <https://doi.org/10.1002/mop.31457>.
- [30] Kumar A, De A, Jain RK. CSRR and open-stub based circular polarized and double band eight-port MIMO antenna for 5G and ISM band applications. *Microsyst Technol* 2022;28:1727–38. <https://doi.org/10.1007/s00542-022-05316-6>.
- [31] Guo J, Cui L, Li C, Sun B. Side-edge frame printed eight-port dual-band antenna array for 5G smartphone applications. *IEEE Trans Antennas Propag* 2018;66(12): 7412–7. <https://doi.org/10.1109/TAP.2018.2872130>.
- [32] Zhang X, Li Y, Wang W, Shen W. Ultra-wideband 8-port MIMO antenna array for 5G metal-frame smartphones. *IEEE Access* 2019;7:72273–82. <https://doi.org/10.1109/ACCESS.2019.2919622>.
- [33] Palanisamy P, Subramani M. Design and packaging of polarization diversity 3D-UWB MIMO antenna with dual band notch characteristics for vehicular communication applications. *AEU-Int J Electron C* 2021;138:153869.
- [34] Xia Y-Q, Chen X-R, Tang T. A novel eight ports dual band antenna array for 2.4/3.5GHz MIMO applications. *Optik* 2015;126(11–12):1175–80.
- [35] Zeng W-F, Chu Q-X. Eight-element fifth-generation multiple-input multiple-output antenna designed by modal currents cancellation. *Int J RF Microw Comput Aided Eng* 2022;32(9):e23254.
- [36] Cheng J. Novel twelve port eight element UWB-MIMO antenna. *Microwave Opt Technol Lett* 2021;63:1935–41. <https://doi.org/10.1002/mop.32848>.
- [37] Addepalli T, Desai A, Elfergani I, Anvesh Kumar N, Kulkarni J, Zebiri C, et al. 8-port semi-circular arc MIMO antenna with an inverted L-strip loaded connected ground for UWB applications. *Electronics* 2021;10:1476. <https://doi.org/10.3390/electronics10121476>.
- [38] Balanis CA. Antenna theory: analysis and design. 3rd ed. Hoboken, NJ, USA: Wiley; 2005. p. 811–20.
- [39] Blanch S, Romeu J, Corbella I. Exact representation of antenna system diversity performance from input parameter description. *Electron Lett* 2003;39(9):705–7.
- [40] Tian R, Lau BK, Ying Z. Multiplexing efficiency of MIMO antennas. *IEEE Antennas Wireless Propag Lett* 2011;10:183–1866.
- [41] Manteghi M, Samii YR. Multiport characteristics of a wideband cavity backed annular patch antenna for multi polarization operations. *IEEE Trans Antennas Propag* 2005;53(1):466–74.



Muhammad Irshad Khan received the B.Sc. (Hons.) degree in Electrical Electronic engineering from the Comsats Institute of Information Technology Abbottabad, Pakistan, and the M.S in Electrical engineering from the Capital University of Science and Technology, Islamabad, Pakistan in 2016. He received his Ph.D. degree in electrical engineering from the University of Engineering and Technology, Peshawar, Pakistan in 2021. He is currently working as a Postdoctoral Research fellow at the College of electronics and information engineering, Nanjing University of Aeronautics and Astronautics (NUAA), Nanjing, China. His research interests include microwave and RF circuit design. UWB antenna design and analysis, Meta-material absorbers, MIMO antennas, Microwave filters, Beam steering antennas and reconfigurable antennas.



Shaobin Liu (Member, IEEE) received the Ph.D. degree in electronics science and technology from the National University of Defense Technology, Changsha, China, in 2004. He is currently a Professor of electromagnetic and microwave technology with the Nanjing University of Aeronautics and Astronautics, Nanjing, China. His research focuses on plasma stealthy antennas, microwave, radio frequency, and electromagnetic compatibility.



Jianliang Mao received the B.Sc., M.Sc., and Ph.D. degrees from the School of Automation, Southeast University, Nanjing, China, in 2011, 2014, and 2018, respectively. From 2018 to 2021, he worked at the Research and Development Institute, Estun Automation Co., Ltd. He was selected into “Jiangsu Province entrepreneurship and innovation plan” in 2019. He is currently with the College of Automation Engineering, Shanghai University of Electric Power. His research interests include model predictive control, sliding mode control, vision based interactive control and their applications to electric drives and robot manipulators.



Abdul Basit received his BSc degree in Electrical Engineering in 2012 from University of Engineering and Technology Peshawar, Pakistan, the MSc degree in 2015 from CECOS University of IT and Emerging Sciences Peshawar, Pakistan, and the PhD degree in Electrical Engineering from University of Engineering and Technology Peshawar, Pakistan in 2021. From 2013 to 2017, he served as Lecturer in the Department of Electrical Engineering University of Engineering and Technology Bannu campus, Pakistan. From 2017 to 2018, he served as an Assistant Director (Technical) in NTDC (National Transmission and Dispatch Company) Pakistan. Nowadays he is working as a postdoctoral scientific researcher at Ningbo Institute of Technology, Zhejiang University, China. His research interests are mainly in the design of microwave filters, power integrated differential controller, antenna design at millimeter-wave and terahertz applications etc.



Amil Daraz was born in Pakistan, in 1989. He received, the B.E. degree in Electronics Engineering from COMSATS University Islamabad, Pakistan in 2012, the M.S. degree in Power and Control Engineering from International Islamic University Islamabad (IIUI), Pakistan, and Ph.D degree in Electrical Engineering from International Islamic University Islamabad (IIUI), Pakistan. He is currently pursuing his Postdoctoral research at NingboTech University, Ningbo, China. His research interests include control systems, Power system operation and Control, optimization of solving nonlinear problems.



Afzal Ahmed received his BS (Computer Engineering) and MS (Electrical Engineering) from COMSATS University Islamabad, Lahore Campus and COMSATS University Islamabad, Abbottabad Campus, Pakistan in 2013 and 2017, respectively. Currently, he is a doctoral student in College of Electronics and Information Engineering Nanjing University of Aeronautics and Astronautics, China. His research interests include metamaterials and antennas.